Journal of Psychiatric Research 82 (2016) 30–39

Contents lists available at ScienceDirect

Journal of Psychiatric Research

journal homepage: www.elsevier.com/locate/psychires

Frequency-specific alterations in functional connectivity in treatment-resistant and -sensitive major depressive disorder

Zongling He [a, b], Qian Cui [c], Junjie Zheng [a], Xujun Duan [a], Yajing Pang [a], Qing Gao [a], Shaoqiang Han [a], Zhiliang Long [a], Yifeng Wang [a], Jiao Li [a], Xiao Wang [a], Jingping Zhao [d], Huafu Chen [a, *]

[a] Center for Information in BioMedicine, Key Laboratory for Neuroinformation of Ministry of Education, School of Life Science and Technology, University of Electronic Science and Technology of China, Chengdu 610054, China
[b] Mental Health Center, The Fourth People's Hospital of Chengdu, Sichuan 610000, China
[c] School of Political Science and Public Administration, University of Electronic Science and Technology of China, Chengdu 610054, China
[d] Mental Health Institute, The Second Xiangya Hospital, Central South University, Changsha, Hunan 410011, China

ARTICLE INFO

Article history:
Received 23 January 2016
Received in revised form
8 July 2016
Accepted 8 July 2016

Keywords:
Major depressive disorder
Treatment-resistant depression
Treatment-sensitive depression
Functional connectivity
Resting state
Functional magnetic resonance imaging

ABSTRACT

Major depressive disorder (MDD) may involve alterations in brain functional connectivity in multiple neural circuits and present large-scale network dysfunction. Patients with treatment-resistant depression (TRD) and treatment-sensitive depression (TSD) show different responses to antidepressants and aberrant brain functions. This study aims to investigate functional connectivity patterns of TRD and TSD at the whole brain resting state. Seventeen patients with TRD, 17 patients with TSD, and 17 healthy controls matched with age, gender, and years of education were recruited in this study. The brain was divided using an automated anatomical labeling atlas into 90 regions of interest, which were used to construct the entire brain functional networks. An analysis method called network-based statistic was used to explore the dysconnected subnetworks of TRD and TSD at different frequency bands. At resting state, TSD and TRD present characteristic patterns of network dysfunction at special frequency bands. The dysconnected subnetwork of TSD mainly lies in the fronto-parietal top-down control network. Moreover, the abnormal neural circuits of TRD are extensive and complex. These circuits not only depend on the abnormal affective network but also involve other networks, including salience network, auditory network, visual network, and language processing cortex. Our findings reflect that the pathological mechanism of TSD may refer to impairment in cognitive control, whereas TRD mainly triggers the dysfunction of emotion processing and affective cognition. This study reveals that differences in brain functional connectivity at resting state reflect distinct pathophysiological mechanisms in TSD and TRD. These findings may be helpful in differentiating two types of MDD and predicting treatment responses.

1. Introduction

Major depressive disorder (MDD) is a prevalent mental disorder characterized by persistent prevailing low mood and withdrawal from pleasurable activities (Minor et al., 2005). Patients with MDD suffer impairment in domains of emotional processing, cognitive control, affective cognition (cognitive control of emotion), and reward processing (Disner et al., 2011, Kerestes et al., 2014). MDD is one of the top public health concerns worldwide and causes significant disability and disease burden. Although numerous studies have focused on treatments for MDD, approximately one-third of patients with MDD fail to respond to antidepressants and are considered "treatment resistant" (Ionescu et al., 2015).

Previous neurobiological studies confirmed the occurrence of failure on mechanisms for serotonin reuptake inhibition in treatment-resistant depression (TRD) (Coplan et al., 2014) and is regarded as the basis of responses to antidepressant treatments. Changes may be correlated with genetic and biological factors, such as polymorphism of the serotonin transporter gene (Coplan et al., 2014; Santos et al., 2015). Therefore, the pathological mechanism of TRD may differ from that of treatment-sensitive depression (TSD); however, reliable biomarkers used to effectively predict

* Corresponding author.
E-mail address: chenhf@uestc.edu.cn (H. Chen).

http://dx.doi.org/10.1016/j.jpsychires.2016.07.011
0022-3956/

treatment responses and identify two subtypes of depression are lacking (Jentsch et al., 2015).

Functional magnetic resonance imaging (fMRI) techniques are used to investigate the pathophysiology of MDD and identify biomarkers, which can be used to predict treatment responses. To date, the majority of fMRI studies have employed stimulus-driven paradigms, in which certain local brain functional abnormalities are found during cognitive or affective processing. The most consistent findings in MDD studies include decreased frontal cortex activity [primarily involving medial prefrontal cortex (MPFC) and dorsolateral prefrontal cortex (DLPFC)], as well as increased limbic system activity [including anterior cingulate cortex (ACC), amygdala, and hippocampus]at tasking state (Disner et al., 2011; Kerestes et al., 2014; Murray et al., 2011). For example, hyperactivity of amygdala and altered connectivity between the amygdala and ACC were probed under negative emotional face stimuli in MDD (Kerestes et al., 2014; Mingtian et al., 2012).

fMRI is employed in a "stimulus-free" manner, such as in the case of resting state, to reflect the intrinsic activity patterns of brain (Barkhof et al., 2014). A hypothesis proposes that MDD is associated with dysregulated neural networks, rather than disruption of single brain regions (Gong and He, 2015; Palazidou, 2012). Alterations in brain networks, including default mode network (DMN), salience network (SN), cognitive control network (CCN), and affective network (AN), have been identified in MDD (Guo et al., 2014, Kaiser et al., 2015, Luo et al., 2015, Wang et al., 2012, Zeng et al., 2012). Previous studies on functional connectivity (FC) within and between these networks at resting state showed that MDD exhibits hypoconnectivity within the CCN network, which is mainly composed of DLPFC and parts of the parietal lobe and involved in achieving goal-relevant stimuli, regulation of cognitive process, and top-down regulation of attention and emotion (Dichter et al., 2015, Ruge and Wolfensteller, 2015). MDD is also associated with hyperconnectivity within the DMN, which contains several brain regions located in the center of the brain, such as ACC, MPFC, and posterior cingulate cortex (PCC)/precuneus regions. This network is possibly involved in episodic memory and internally oriented, self-referential thought (Guo et al., 2014; Marchetti et al., 2012). Between networks, brain regions belonging to DMN exhibit hyperconnectivity with CCN and SN (insula) (Sawaya et al., 2015). Finally, another robust neuropathology patterns have gained increased research attention. The dysregulation of cortical–limbic–subcortical circuit (sometimes named as affective network, AN) is assumed to perform a vital role in the pathogenesis of depression (Maletic and Raison, 2014; Wang et al., 2012). Furthermore, structures in limbic and subcortical areas show abnormal activation in MDD; these structures include medial thalamus, amygdala, striatum, and hippocampus/parahippocampal, which are possibly involved in emotional perception and function in neural responses to negative stimuli. Cortical regions, such as ACC, and ventromedial prefrontal cortex (vMPFC), are thought to perform a regulatory role over limbic structures, which process emotional stimuli. A breakdown in this circuit could be related to deficits of mood regulation (Maletic and Raison, 2014; Palazidou, 2012). Several studies on MDD reported decreased functional connectivity between ACC and amygdala, pallido striatum, and thalamus (Anand et al., 2009). Decreased functional connectivity between the ACC and a number of cortical areas, including MPFC, superior and inferior frontal cortices, and insula, have also been reported in MDD (Gong and He, 2015; Wang et al., 2016). These findings suggest that MDD may involve alterations in brain connectivity in multiple neural circuits and exhibit large-scale network dysfunction.

Studies have investigated the involvement of alterations in brain function in MDD in responses to antidepressant treatments. For example, TRD shows robust decreased regional homogeneity (ReHo) in the prefrontal cortex and increased ReHo in limbic regions, as well as decreased connectivity within cortical–limbic circuits relative to TSD (Lui et al., 2011, Wu et al., 2011). Furthermore, successful antidepressant treatment of MDD results in increased connectivity among PFC, ACC, and limbic regions (thalamus, striatum, and amygdala) (Anand et al., 2007). By contrast, higher amplitude of low-frequency fluctuations and hyperconnectivity within the DMN was found in TRD relative to TSD. In certain studies, hyperconnectivity within the DMN was normalized in MDD after successful treatment (Guo et al., 2012, Li et al., 2013, Posner et al., 2013). In addition, low connectivity within the CCN predicts poor antidepressant outcomes in MDD (Alexopoulos et al., 2012). However, most previous studies used traditional FC analysis and preselected smaller regions of interest, thereby complicating the process of describing the pattern of brain FC at the whole-brain scale.

In this study, we investigated FC alterations in TSD and TRD by using an analysis method, called network-based statistic (NBS) (Zalesky et al., 2010). NBS is a powerful method when performing this kind of analysis. And can be thought of as a translation of conventional cluster statistics to a graph. NBS differs from cluster-based statistical methods used in mass univariate testing. Rather than in physical space, NBS clusters in topological space, where the most basic equivalent of a cluster is a connected graph component. Hence, FC alterations are identified and modeled as a network. Furthermore, NBS can offer substantially greater power than generic procedures for controlling family-wise error rate (Zalesky et al., 2010). Moreover, recent studies indicate that different frequency bands contribute differently to the low-frequency oscillations (LFOs), and frequency-dependent changes in LFOs have been reported in various brain disorders (Yu et al., 2014). Previous studies have suggested that the functional connectivity abnormalities in spontaneous low frequency (0.01–0.08 Hz) oscillations, but without detailedly description the functional connectivity abnormalities in more narrow frequency bands, for example, slow4 (0.027–0.073 Hz) and slow5 (0.01–0.027 Hz). Zuo have found that LFO amplitudes in slow4 were higher than in the slow5 in many brain regions, such as the basal ganglia, thalamus, and precuneus (Zuo et al., 2010). Han and his colleague (Han et al., 2011) found that amnestic mild cognitive impairment patients have widespread abnormalities in intrinsic brain activity depend on the difference ALFF/fALFF activities in the slow4 and slow5, Luo et al. found major depression disorder patients have abnormal brain network connectivity in different frequency bands (Luo et al., 2015). Indeed, frequency-dependent changes have been found in many diseases (Yu et al., 2014). However, no research focus on the functional connectivity abnormality in slow4 and slow5 based on NBS. Therefore, in the current study, we directly tested whether MDD-related changes in large-scale brain connectivity are dependent on frequency. This exploration will be helpful in discovering neural mechanisms underlying the MDD and provide additional information to improve understanding of the neurobiology of this disorder.

2. Methods

2.1. Subjects

A total of 35 right-handed patients with MDD were recruited from the Mental Health Institute, the Second Xiangya Hospital, Central South University, China. All patients were interviewed by two experienced psychiatrists using the Structured Clinical Interview for DSM-IV-TR-Patient Edition (SCID-P, 2/2001 revision, Biometrics Research Department, New York State Psychiatric Institute, USA, Web page: http://www.scid4.org/). DSM-IV criteria for MDD

were used for diagnosis. Exclusion criteria include schizophrenia, bipolar disorder, anxiety disorders, and other psychotic disorders, mental retardation or personality disorder, any history of loss of consciousness, substance abuse, serious medical or neurological illness, and age younger than 18 years or older than 50 years. The severity of depression was assessed using the 17-item Hamilton Depression scale (HAMD), and only patients who scored 18 or higher were included.

Eighteen patients with MDD suffered from TRD. Treatment resistance is defined as non-responsiveness to a minimum of two adequate trials [in terms of dosage, duration (6 weeks for each trial), and compliance] of different classes of antidepressants. Non-responsiveness is defined as a less than 50% reduction in HAMD score. Data from one subject were excluded because of excessive head motion during fMRI scan.

Seventeen patients with MDD suffered from TSD, characterized as first-episode and treatment-naive. Following the fMRI scan, all patients were directed to take antidepressants for 6 weeks. The reduction in HAMD score after antidepressant treatment exceeded 50%.

The drugs administered included one of the three typical classes of antidepressants: tricyclic antidepressants, selective serotonin reuptake inhibitors (SSRI), and serotoninnorepinephrine reuptake inhibitors (SNRI).

Eighteen right-handed healthy controls (HC), which were recruited from the community through poster advertisement, were also interviewed using the Structured Clinical Interview for DSM-IV (non-patient edition). None of the HCs presented a history of serious medical or neuropsychiatric illness or a family history of major psychiatric or neurological illness in their first-degree relatives. Data from one subject were excluded because of excessive head motion during fMRI scan.

Clinical and demographic data from the remaining 52 participants are shown in Table 2. The three groups were well-matched in age, gender, and years of education. All subjects were given information on the procedure and provided written informed consent approved by the Ethics Committee of the Second Xiangya Hospital, Central South University.

2.2. Scan acquisition

Imaging was performed on a 1.5T GE scanner (General Electric, Fairfield, Connecticut, USA). A head coil fitted with foam padding was used to minimize head movement. Patients were informed to remain motionless, keep their eyes closed, and not think of anything in particular. The following parameters were used for T1 anatomical imaging axially: repetition time/echo time (TR/TE) of 1924/7.5 ms, 20 slices, 256 × 256 matrix, 90° flip angle, 24 cm field of view (FOV), 5 mm section thickness, and 1 mm gap. Functional images were acquired at the same locations as anatomical slices by using an echo-planar imaging sequence with the following parameters: TR/TE of 2000/40 ms, 20 slices, 64 × 64 matrix, 90° flip angle, 24 cm FOV, 5 mm section thickness, and 1 mm gap. For each participant, the fMRI scan lasted for 6 min, and 180 vol were obtained. Data from 2 subjects (1 patient and 1 control) were discarded due to excessive head movement (translational movement >1.5 mm or rotation > 1.5°).

2.3. Data preprocessing

All preprocessing steps were conducted using Statistical Parametric Mapping version 8 (SPM8, http://www.fil.ion.ucl.ac.uk/spm/) and DPARSF software (http://www.restfmri.net/forum/). Images of the first 10 vol were discarded to stabilize the scanner and subjects to adapt to the environment. The remaining 170 functional scans were first corrected for within-scan acquisition time differences between slices and then realigned to the middle volume to correct for inter-scan head motions. Subsequently, fMRI images were spatially normalized to a standard template (Montreal Neurological Institute) and resampled to 3 mm × 3 mm × 3 mm. After normalization, the blood oxygenation level-dependent (BOLD) signal of each voxel was first detrended to abandon the linear trend. Temporal band-pass filtering was then performed in the following two frequency bands: 0.01–0.027 Hz (termed as slow5) and 0.027–0.073 Hz (termed as slow4). Finally, nuisance covariates, including six head motion parameters, cerebrospinal fluid signals, and white matter signals, were regressed from BOLD signals. We did not regress the global signal in this study because several studies reported that this controversial step could lead to false-positive results (Saad et al., 2012).

2.4. Network construction

An automated anatomical labeling (AAL) atlas was employed to divide the brain into 90 regions of interest (ROI) and construct whole-brain functional networks. For each subject, the representative time series of each individual region was obtained by averaging the fMRI signals over all voxels in this region. FC between each pair of regions was evaluated using Pearson's correlation coefficients. Finally, a 170 × 90 × 90 3D time series matrix was acquired. In this study, we constructed brain networks, where nodes represented brain regions and edges represented inter regional resting-state FC. These functional connections were used in subsequent analyses. (see Table 1 and Fig. 1).

2.5. Statistical analysis

To localize the specific circuits where functional connectivity was altered in the patients, we used the NBS approach (Zalesky et al., 2010, 2012, 2011). In NBS procedures, we firstly identified connections in network as significantly changed connections by a supra threshold which in this study was presented by two-sample *t*-test t values or analysis of variance (ANOVA) F values. Then, in these survived connections, any directly or indirectly connected links or connections were formed a components. The numbers of links in a component was the size of it. Next, a total of N random permutation testing was used to describe a p value of each component on its size. The permutation testing was performed independently, the group to which each subject belongs is randomly exchanged. For each permutation, the test statistic value is recalculated, after which the same threshold was applied to define a set of supra threshold links. The maximal component size in the set of supra threshold links derived from each of the permutation. Permutations is then determined and stored, there by yielding an empirical estimate of the null distribution of maximal component size. Finally, the p-value of an observed component of size k is estimated by finding the total number of permutations for which the maximal component size is greater than k and normalizing by N. This kind of permutation testing is more or less synonymous with conventional cluster-based thresholding of statistical parametric maps. The method could be used to control the family-wise error rate (FWER) of identified components. The p values < 0.05 was set as the significant level of the components in this permutations test.

In this study, we first used the NBS method to determine significantly abnormal FC circuits in three groups (TRD, TSD, HC) in both slow-4 and slow-5 frequencies. Significantly changed components were identified by NBS significant level at $p < 0.05$ with individual connectivity statistic F > 6 (by one-way ANOVA test, $p < 0.005$). We then tested significantly changed connections

Table 1
Regions of automated anatomical labeling (AAL) atlas and anatomy of the cerebral cortex.

Regions	Abbreviation	Anatomy of the cerebral cortex
Prefrontal lobe		
Superior frontal gyrus (dorsal)	SFGdor	Dorsolateral prefrontal cortex
Middle frontal gyrus	MFG	Dorsolateral prefrontal cortex
Inferior frontal gyrus (triangular)	IFGtriang	Dorsolateral prefrontal cortex
Inferior frontal gyrus (opercula)	IFGoperc	Dorsolateral prefrontal cortex
Superior frontal gyrus (medial)	SFGmed	Medial prefrontal cortex
Orbitofrontal cortex (medial)	ORBmed	Medial prefrontal cortex
Rectus gyrus	REC	Orbital prefrontal cortex
Orbitofrontal cortex (superior)	ORBsup	Orbital prefrontal cortex
Orbitofrontal cortex (middle)	ORBmid	Orbital prefrontal cortex
Orbitofrontal cortex (inferior)	ORBinf	Orbital prefrontal cortex
Olfactory	OLF	Orbital prefrontal cortex
Other parts of frontal lobe		
Rolandic operculum	ROL	Frontal-temporal-parietal operculum
Supplementary motor area	SMA	Superolateral frontal cortex
Precentral gyrus	PreCG	Superolateral frontal cortex
Paracentral lobule	PCL	Medial/inferior frontal cortex
Parietal lobe		
Supramarginal gyrus	SMG	Lateral parietal cortex
Inferior parietal lobule	IPL	Lateral parietal cortex
Angular gyrus	ANG	Lateral parietal cortex
Precuneus	PCUN	Medial/inferior parietal cortex
Superior parietal gyrus	SPG	Superolateral parietal cortex
Postcentral gyrus	PoCG	Superolateral parietal cortex
Temporal lobe		
Superior temporal gyrus	STG	Lateral temporal cortex
Middle temporal gyrus	MTG	Lateral temporal cortex
Inferior temporal gyrus	ITG	Lateral temporal cortex
Temporal pole (superior)	TPOsup	Lateral temporal cortex
Temporal pole (middle)	TPOmid	Lateral temporal cortex
Heschl gyrus	HES	Lateral temporal cortex
Fusiform gyrus	FFG	Medial temporal cortex
Occipital lobe		
Superior occipital gyrus	SOG	Medial/inferior occipital cortex
Middle occipital gyrus	MOG	Medial/inferior occipital cortex
Inferior occipital gyrus	IOG	Medial/inferior occipital cortex
Lingual gyrus	LING	Medial/inferior occipital cortex
Cuneus	CUN	Medial/inferior occipital cortex
Calcarine cortex	CAL	Medial occipital cortex
Limbic		
Posterior cingulate gyrus	PCG	Limbic region
Middle cingulate gyrus	MCG	Limbic region
Anterior cingulate gyrus	ACG	Limbic region
Parahippocampal gyrus	PHG	Limbic region
Hippocampus	HIP	Limbic region
Amygdala	AMYG	Limbic region
Insula	INS	Limbic region
Subcortical		
Pallidum	PAL	Corpus striatum
Caudate	CAU	Corpus striatum
Putamen	PUT	Corpus striatum
Thalamus	THA	Subcortical region

within these circuits between groups. The significantly changed components between groups were identified by NBS significant level at $p < 0.05$ with individual connectivity statistic $T > 3.25$ (by two-sample t-test, $p < 0.005$). Finally, the functional connectivity z-values of each links in significant components were extracted in the patient group to determine the association between functional connectivity and clinical characteristics (HAMD score, age of first episode, and illness duration). Partial correlations were analyzed, with age, sex, and years of education as confounding factors.

3. Results

3.1. Demographic and clinical characteristics

Seventeen patients with TRD, 17 patients with TSD, and 17 HCs completed the study. Demographic information and clinical characteristics are presented in Table 2. No significant difference in age (ANOVA, $F = 0.81$, $P = 0.451$), gender (Chi-square test, Chi-square value $= 0$, $P = 1$), years of education (ANOVA, $F = 1.53$, $P = 0.236$) was found among the three groups. Moreover, patient groups did not differ significantly in HAMD scores (t-test, $T = -0.92$, $P = 0.363$) and age of first episode (t-test, $T = -1.22$, $P = 0.236$). However, the TRD group had longer illness duration (t-test, $T = 2.83$, $P = 0.012$) than the TSD group.

3.2. Frequency-specific alterations in functional connectivity at resting state

3.2.1. Dysconnected subnetwork: patients with TSD versus HCs

At frequency bands of 0.01–0.027 Hz (slow5), NBS identified a dysconnected subnetwork ($P < 0.001$, correlated) in the TSD group. The dysconnected subnetwork comprised 10 regions and 9 reduced

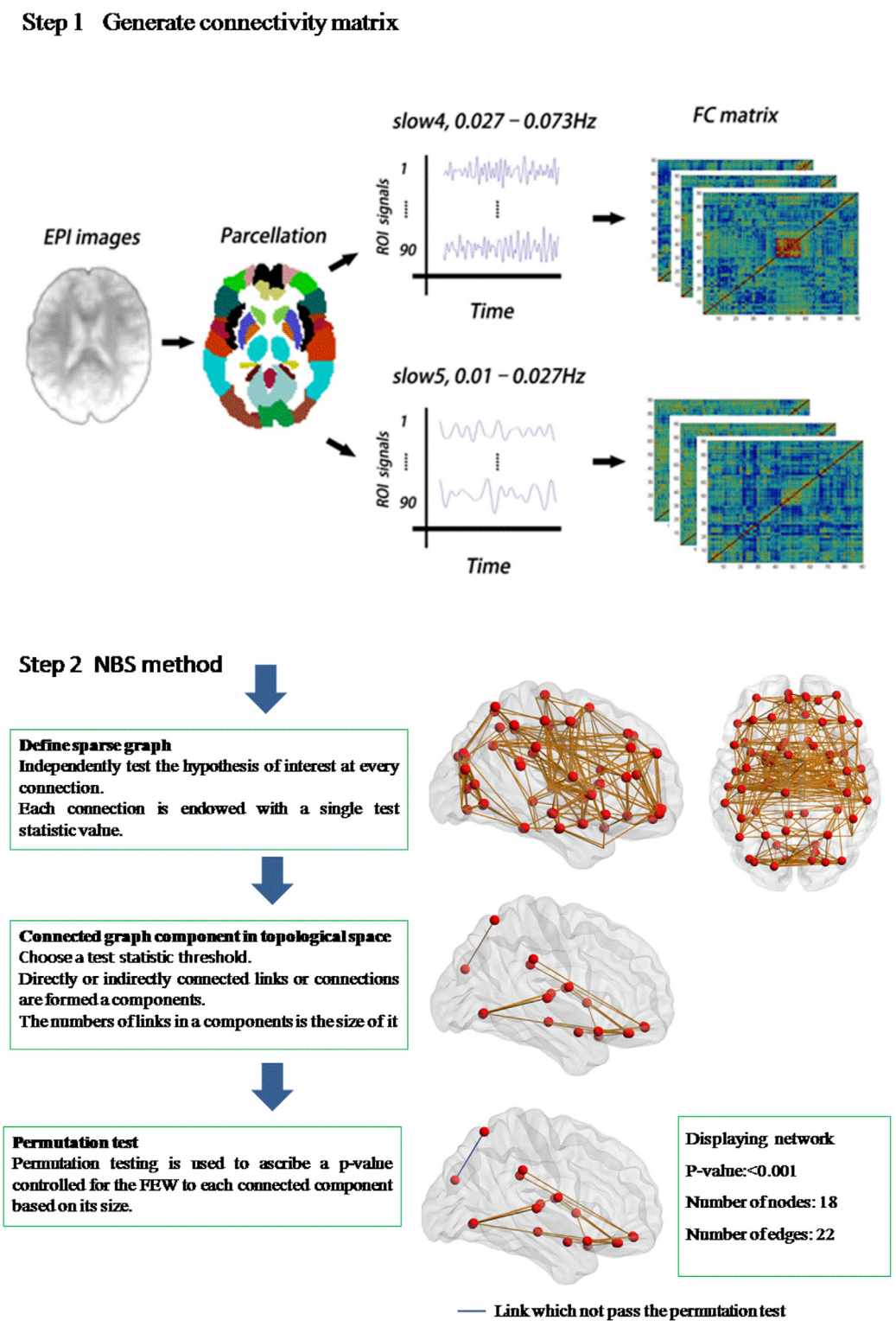

Fig. 1. Flowchart of methods pipeline: overview of data processing and analysis pipeline. Step 1: Resting-state fMRI data were corrected for a temporal shift in acquisition (slice timing), realigned to the middle slice, normalized to an EPI template, detrended, and band pass filtered (0.01–0.027 Hz and 0.027–0.073 Hz). The six head-motion parameters, as well as the white matter and cerebrospinal fluid signals, were regressed out from each voxel's time course. Time courses were extracted for the 90 cerebral regions comprising the automated anatomical labeling (AAL) template and the extent of dependency between every pair of regions was represented at the subject level with a 90 × 90 connectivity matrix. Step 2: network-based statistics process on connectivity. We firstly performed statistics on individual connection in brain network; Then the significant connections survived the threshold t values by *t*-test or F values by ANOVA test were collected and formed components (step 2 Fig. 2); the sizes of components were recorded; Finally, the permutation test was performed to describe a significant level of the components. The survived (permutation test $p < 0.05$) component was identified as significant connections (step 2 Fig. 3 yellow edges). The blue edge (step 2 Fig. 3) was the component which was not significant after NBS correction. (For interpretation of the references to colour in this figure legend, the reader is referred to the web version of this article.)

Table 2
Demographic information and characteristics of patients with TRD or TSD and healthy control (HC).

Variables (Mean ± SD)	TRD	TSD	HC	*P* value
N (M/F)	17 (10/7)	17 (10/7)	17 (10/7)	1.000[b]
Age (years)	26.88 + 7.66	26.72_7.72	24.24 + 4.41	0.451[a]
Education (years)	13.76 + 3.59	12.35 + 2.12	13.82 + 2.38	0.236[a]
Illness duration (months)	37.41 + 50.73	2.59 + 1.32		0.012[c,*]
Age of first episode (years)	23.76 + 6.21	26.71 + 7.28		0.236[c]
HAMD score	23.94 + 3.79	25.59 + 6.31		0.363[c]
Medication state prior to entering study (treatment/treatment-naïve)	15/2	0/17		
Medication (The number of cases, average dosage)				
escitalopram	4 (17.5 mg/d)	3 (18 mg/d)		
fluoxetine	2 (45 mg/d)	2 (40 mg/d)		
paroxetine	5 (45 mg/d)	7 (40 mg/d)		
sertraline	3 (180 mg/d)	4 (180 mg/d)		
venlafaxine	2 (175 mg/d)	1 (175 mg/d)		
amitriptyline	1 (200 mg/d)	0		

*: $p < 0.05$.
[a] by one way ANOVA.
[b] by Chi-square test.
[c] by independent-sample *t*-test.

dysconnections (Fig. 2). The subnetwork encompassed the bilateral inferior parietal lobule, right supramarginal gyrus, bilateral precentral gyrus, lateral prefrontal cortex (left middle frontal gyrus, bilateral inferior frontal gyrus (opercula and triangular), left orbitofrontal cortex (superior), and most areas located in the frontoparietal region. At frequency bands of 0.027–0.073 Hz (slow4), no significant dysconnected subnetwork was found. Significant correlation was not found between connectivity strength of the dysconnected subnetwork and clinical characteristics.

3.2.2. *Dysconnected subnetwork: patients with TRD versus HCs*

At frequency bands of 0.01–0.027 Hz (slow5), NBS identified a dysconnected subnetwork ($P < 0.001$, correlated) in the TRD group. The disconnected subnetwork comprised 18 regions and 22 reduced functional connections (Fig. 3A). The network encompassed the bilateral rectus gyrus, bilateral orbitofrontal cortex (superior), left insula, left hippocampal gyrus, right amygdala, bilateral lingual gyrus, lateral temporal cortex (bilateral superior temporal gyrus, bilateral superior temporal pole, and left Heschl's gyrus), bilateral rolandic operculum, and bilateral supramarginal gyrus. The connectivity strength of the dysconnected subnetwork in the TRD group was found to be negatively correlated with illness duration (Fig. 3A).

At frequency bands of 0.027–0.073 Hz (slow 4), NBS identified a dysconnected subnetwork ($P < 0.001$, correlated) in the TRD group. The subnetwork comprised 14 regions and 15 reduced functional connections (Fig. 3B). The network was centered on bilateral olfactory, which presented reduced FC with right inferior frontal gyrus (triangular and opercula), bilateral rolandic operculum, left Heschl's gyrus, left middle temporal gyrus, left lingual gyrus, bilateral fusiform gyrus, right orbitofrontal cortex (inferior) and rectus gyrus, and left hippocampal gyrus. No significant correlation was found between connectivity strength of the disconnected subnetwork and clinical characteristics.

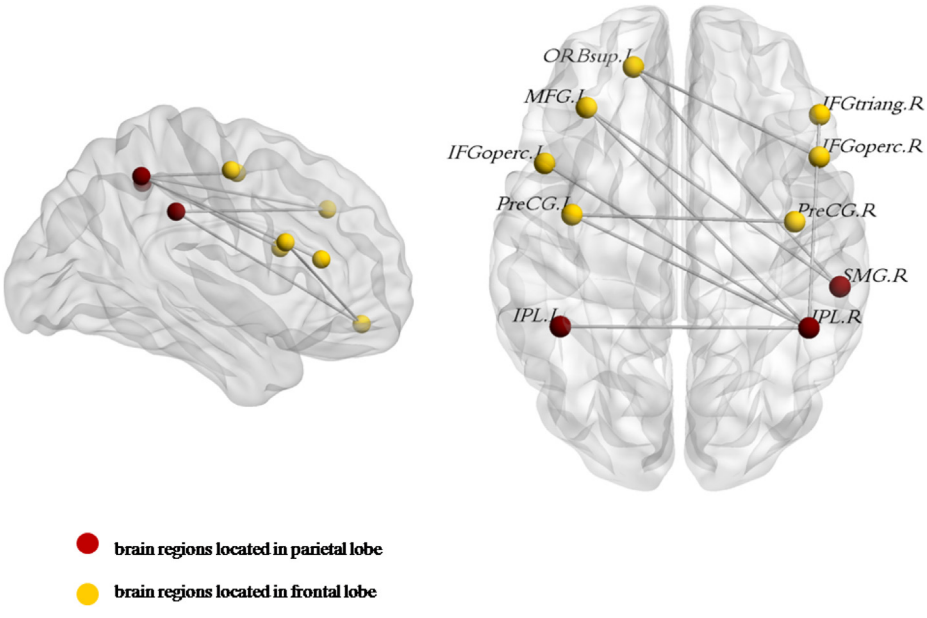

Fig. 2. Dysconnected subnetwork for patients with TSD versus HC. The line show decreased FC. TSD = treatment sensitive depression; HC = healthy control; L: left; R: right; IPL: inferior parietal lobule, SMG: SupraMarginal gyrus; PreCG: precentral gyrus; MFG: middle frontal gyrus; IFGoperc: inferior frontal gyrus (opercula); IFGtriang: inferior frontal gyrus (triangular); ORBsup: orbitofrontal cortex (superior).

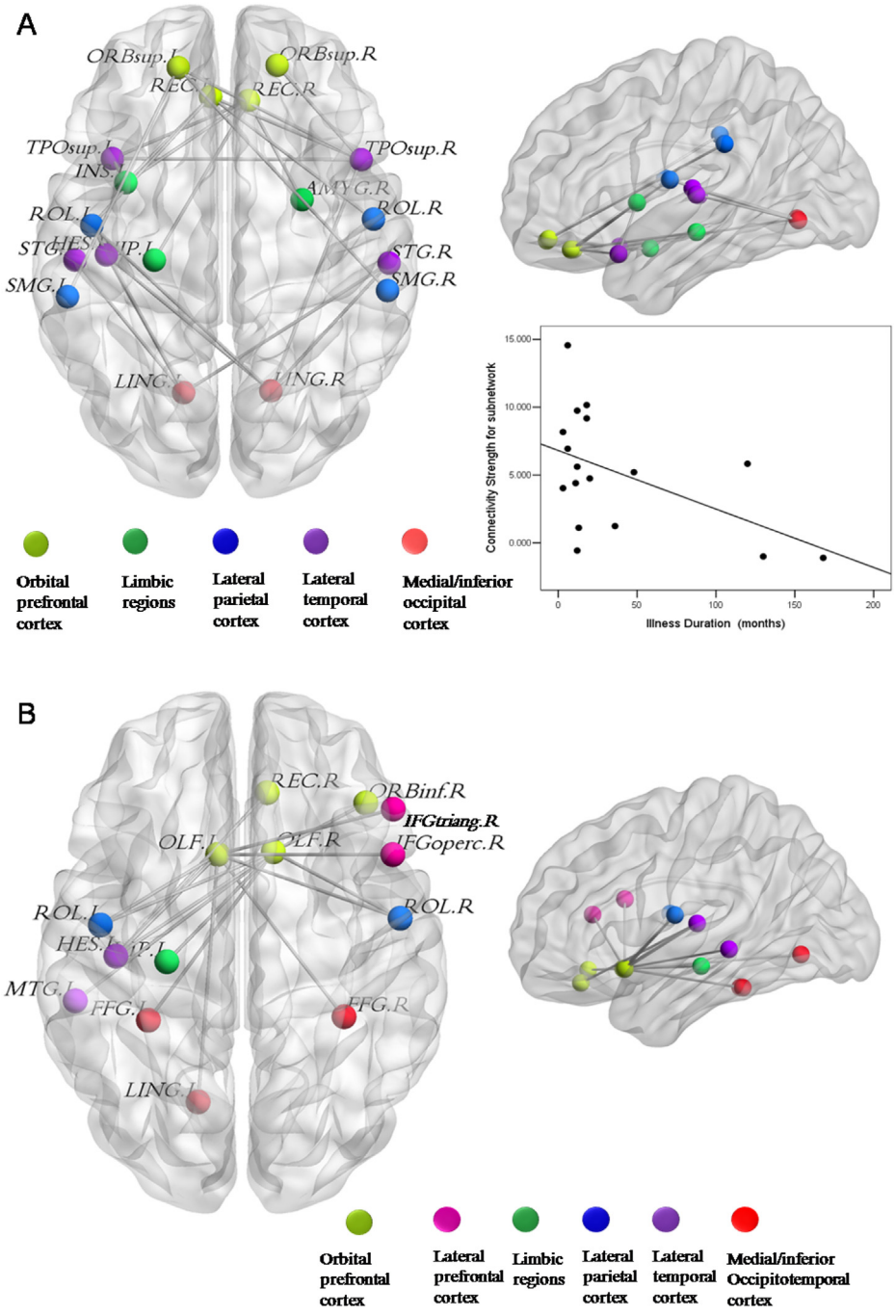

Fig. 3. Dysconnected subnetwork for patients with TRD versus HC. The line show decreased FC. TRD = treatment resistant depression; HC = healthy control; L: left; R: right; ORBsup: orbitofrontal cortex (superior); ORBinf: orbitofrontal cortex (inferior)s; REC: rectus gyrus; INS: insula; HP: hippocampus; AMYG: amygdale; HES: hechl gyrus; STG: superior temporal gyrus; MTG: middle temporal gyrus; TPOsup: superior temporal pole; OLF: olfactory; IFGtriang: inferior frontal gyrus (triangular); IFGoperc: inferior frontal gyrus (opercula); ROL: rolandic operculum; SMG: supramarginal gyrus; FFC: fusiform gyrus; LING: lingual gyrus. A: At the frequency band of 0.01–0.027 Hz; B: At the frequency band of 0.027–0.073 Hz.

3.2.3. *Dysconnected subnetwork: patients with TRD versus patients with TSD*

NBS identified a single dysconnected subnetwork ($P < 0.001$, correlated) in the TRD group at frequency bands of 0.01–0.027 Hz (slow5) compared with that in the TSD group. The subnetwork comprised five regions and four reduced functional connections (Fig. 4). The network encompassed the left parahippocampal gyrus, left precuneus, left posterior cingulate gyrus, left inferior parietal lobe, and right caudate. At frequency bands of 0.027–0.073 Hz (slow 4), NBS identified two dysconnected subnetwork in TRD (Fig. 4). One subnetwork included three reduced connections ($P < 0.001$, corrected), which encompassed left parahippocampal gyrus, bilateral Heschl's gyrus, and left rectus gyrus. The other subnetwork included eight reduced connections ($P < 0.001$, corrected) centered on the bilateral olfactory, which was dysconnected with bilateral inferior occipital gyrus, left fusiform gyrus, right superior parietal gyrus, lateral prefrontal cortex [left middle frontal gyrus, right inferior frontal gyrus (triangular)], and the right

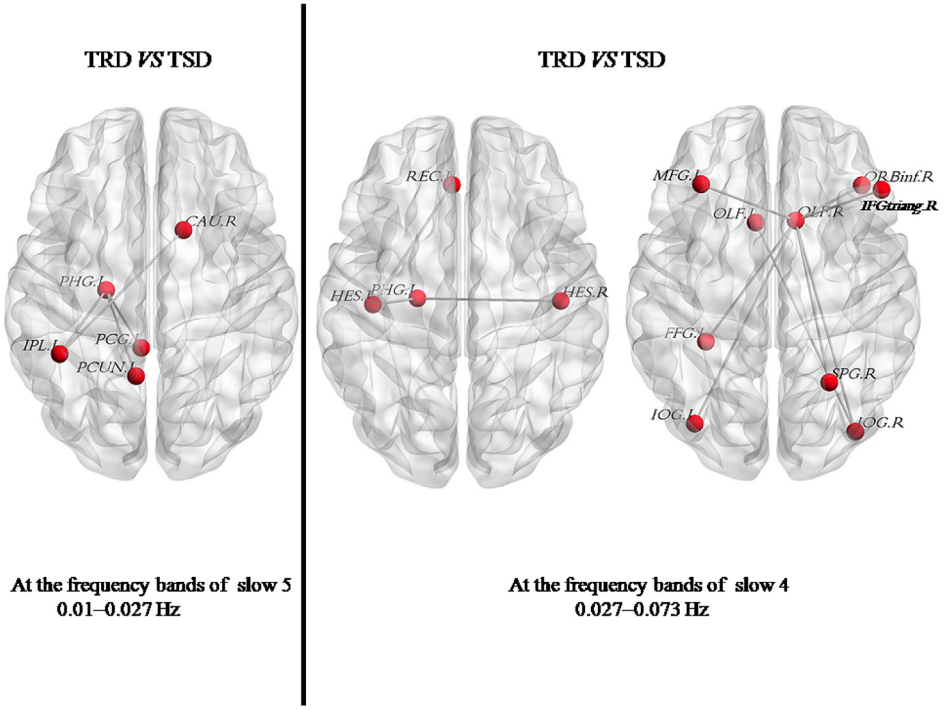

Fig. 4. Dysconnected subnetwork for patients with TRD versus TSD. The line show decreased FC. TRD = treatment resistant depression; TSD = treatment sensitive depression; L: left; R: right; PHG: parahippocampal gyrus; IPL: inferior parietal lobe; PCUN: precuneus, PCG: posterior cingulate gyrus; CAU: caudate; HES: heschl gyrus; REC: rectus gyrus; OLF: olfactory cortex; IOG: inferior occipital gyrus; SPG: superior parietal gyrus, FFG: fusiform gyrus, MFG: middle frontal gyrus; IFGtriang: inferior frontal gyrus (triangular); ORBinf: orbitofrontal cortex (inferior).

orbitofrontal cortex (inferior). No significant correlations were found between connectivity strength of the dysconnected subnetwork and clinical characteristics.

4. Discussion

This study used a new approach, namely, NBS, to identify FC alterations at the resting state of two MDD subtypes, which are modeled as a network. In addition, we directly tested MDD-related changes in large-scale brain connectivity at different frequency bands. In support of previous studies suggesting that MDD may present large-scale network dysfunction, our results showed that brain dysfunction in MDD involves alterations in brain connectivity in multiple neural circuits, as well as depressive symptoms; these symptoms manifest as emotional, cognitive, behavioral, and neuroendocrine disturbances, which correspond to systemic alterations in interconnected brain networks (Kaiser et al., 2015; Palazidou, 2012). Furthermore, this study demonstrated that patients with TSD and TRD showed different dysconnected subnetworks, and aberrant brain FCs were frequency dependent.

At slow 5 (0.01–0.027 Hz), TSD showed a significant dysconnected subnetwork characterized by hypoconnectivity. These dysconnected brain regions are mainly located in the DLPFC and inferior parietal lobule, overlapping with traditional CCN (sometimes called fronto-parietal control network) (Vincent et al., 2008). These networks exhibit coherent activity during task performance and is involved in top-down regulation of attention and emotion, integration of sensory information, and updating of goal-directed behavior (Vincent et al., 2008). Our finding is consistent with those of several previous studies, which showed that MDD exhibits hypoconnectivity within this network, especially between the DLPFC and bilateral posterior parietal cortex (Dichter et al., 2015; Ruge and Wolfensteller, 2015). Abnormal communication within the CCN may stimulate deficits in cognitive control, which are commonly observed in MDD and may contribute to various symptoms, such as difficulty in concentrating or regulating emotions.

TRD showed different significant dysconnected subnetworks at resting state. In this case, dysconnected brain regions are distributed in orbital prefrontal cortex, limbic regions, lateral parietal cortex, lateral temporal cortex, and medial/inferior occipital cortex, which are hypoconnected with one other. The PFC and limbic system (particularly amygdala and hippocampus) are brain structures widely studied in relation to depression (Palazidou, 2012). The PFC lies anteriorly to the premotor and the primary motor area of the frontal cortex, which possess three major sections: (i) dorsolateral aspects (DLPF), (ii) the ventromedial aspects (vMPF), and (iii) orbital aspects (OFC). The DLPFC belongs to CCN and has been implicated in cognitive control and top-down regulation of emotion. vMPFC is necessary for the normal generation of emotions, particularly social emotion. OFC is specifically related to reward processing. Other brain areas implicated in reward processing include ventral striatum, medial PFC, and closely connected regions, including amygdale (Murray et al., 2011). Recent reviews have highlighted the reward processing dysfunction in MDD, which may be associated with key affective and motivational features of MDD (anhedonia) (Whitton et al., 2014). MRI studies have shown a reduction on volume and gray matter density in OFC and hippocampus in depressed patients compared with HCs (Dusi et al., 2015, Klauser et al., 2015, Malykhin and Coupland, 2015). Previous studies also consistently found altered OFC activation in MDD during risky decision-making processes involving monetary rewards (Shad et al., 2011). In a wider range, OFC, hippocampus, and amygdala constitute the complex cortical–limbic–subcortical circuits (Maletic and Raison, 2014); these structures are responsible for maintaining emotional stability and appropriate responses to

emotional stimuli by modulating endogenously generated feeling states, such as melancholic feelings induced by memories of past losses, and externally induced emotional states. This system is also linked with relevant structures in midbrain/brainstem (for example, serotonergic raphe nuclei and adrenergic nucleus coeruleus) and is responsible for regulating neurotransmission and neuroendocrine function (Palazidou, 2012). The present study supports the hypothesis that the balance among structures within this neural circuit is disrupted in the depressed state (Graham et al., 2013, Guo et al., 2015, Palazidou, 2012), especially the aberrant functional connectivity between OFC and amygdala, insula and hippocampus; as a result, the regulatory (inhibitory) action of the PFC on limbic structures is impaired. This dysregulation may be responsible for clinical depressive syndrome and associated autonomic, neuroendocrine disturbances. Furthermore, the dysconnected subnetwork comprise other brain regions referred to the visual recognition circuit (lingual gyrus), auditory information processing (primary auditory cortex, superior temporal gyrus, and Heschl's gyri), and language perception and processing (supramarginal gyrus and rolandic operculum).

Notably, the connectivity strength of this subnetwork is negatively correlated with illness duration. Several factors related to chronic illness duration, such as exposure to antidepressant medication and depressive state for long duration, may be partly responsible for FC alterations. But, depressive disorder is a paroxysmal disease, the illness duration itself may not show the clinical features of the disease well. Some other factors, like the age of the first episode, the frequency of the depression, the time of duration of a single episode, are also likely to have relevance to the brain dysfunction. We haven't had enough information about that during the process of the data collection in our study, so it will surely be helpful to know more about the pathological mechanism of depressive disorder, if collect more precise clinical data in further study.

At slow 4 frequency (0.027–0.073 Hz), TSD showed no significant dysconnected subnetworks, whereas TRD demonstrated one dysconnected subnetwork, which does not completely overlap with that shown at slow 5. The subnetwork is centered on the olfactory cortex and situated in the middle of the OFC. In addition, the subnetwork exhibits hypoconnectivity with other brain regions, referring to visual recognition (lingual gyrus and fusiform gyrus) (Dichter et al., 2015), auditory and language information processing (rolandic operculum and Heschl's gyri), emotional processing (OFC and hippocampus), and cognitive control (DLPFC). The olfactory cortex is not only involved in olfactory perception but present extensive reciprocal connections with emotion areas, including amygdala, hippocampus, and OFC (Krusemark et al., 2013). The olfactory system performs a role in the experience and processing of emotion. Olfactory stimulation can directly increase the activity of amygdala, but olfactory perception is known to be dominated by emotion (Schablitzky and Pause, 2014). This finding indicates that the mood-regulating mechanism, which is mediated by olfactory and olfactory cortex, may be disrupted in TRD but may be intact in TSD. This difference reveals the discrepancy in pathomechanism between TSD and TRD.

Overall, TSD and TRD presented characteristic patterns of network dysfunction at special frequency bands at the resting state. The dysconnected subnetwork of TSD mainly lies in the frontoparietal top-down control network, which reflects that the pathological mechanism of TSD mainly refers to impairment in cognitive control. By contrast, the abnormal neural circuits of TRD is extensive and complex, not only depending on the abnormal affective network but also involving other networks, including SN, auditory network, visual network, and language processing cortex. This finding indicates that dysfunction of emotion processing and affective cognition may be more critical in TRD. Previous genetic and neurobiological research showed that TRD and TSD do not completely present the same pathological aberrances (Ionescu et al., 2015; Santos et al., 2015). Therefore, our findings support the standpoint that TSD and TRD may be triggered by different pathological mechanisms. Furthermore, the aberrant connectivity between components of AN (parahippocampal gyrus, caudate, and rectus gyrus) and other networks, especially DMN (precuneus, posterior cingulate gyrus, and inferior parietal lobe) and auditory network (bilateral Heschl's gyrus), may be the potential endophenotype in predicting treatment responses and differentiating TRD and TSD.

This study presents several limitations. First, small sample size may have reduced the general definitiveness of our results; thus, well-designed studies with a larger sample size are needed. Second, patients with TRD were exposed to antidepressant medication and depressive state for long duration prior to entering study. This exposure does not match that of patients with TSD, thereby making the result confusing. Finally, a follow-up study is needed to clarify the dynamic relationship between depression and significant brain alterations.

Contributors

Design the study: Huafu Chen, Jingping Zhao and Xujun Duan.

Recruit subjects and collect clinical information: Zongling He, Qian Cui, Yajing Pang.

MRI scan and acquire imaging data: Jiao Li, Xiao Wang, Shaoqiang Han, Yifeng Wang.

MRI data preprocessing: Junjie Zheng, Qing Gao and Zhiliang Long.

Data analysis and write the paper: Zongling He, Qian Cui.

Acknowledgments

We thank the 863 project (2015AA020505), the 973 project (2012CB517901), the Natural Science Foundation of China (61533006 and 31400901), the Fundamental Research Funds, and the Scientific research project of Sichuan Medical Association (S15012), which provided the funding for collecting data, paying remuneration and traffic expenditures fee to participants; the Youth Innovation Project of Sichuan Provincial Medical Association (Q14014), the Science Foundation of Ministry of Education of China (14XJC190003), which provided the funding to buy computer and software for data processing; and thank the Fundamental Research Funds for the Central Universities (ZYGX2014J104), which provided the funding for data analyzing and English proofing.

References

Alexopoulos, G.S., Hoptman, M.J., Kanellopoulos, D., Murphy, C.F., Lim, K.O., Gunning, F.M., 2012. Functional connectivity in the cognitive control network and the default mode network in late-life depression. J. Affect Disord. 139, 56–65.

Anand, A., Li, Y., Wang, Y., Gardner, K., Lowe, M.J., 2007. Reciprocal effects of antidepressant treatment on activity and connectivity of the mood regulating circuit: an FMRI study. J. Neuropsychiatry Clin. Neurosci. 19, 274–282.

Anand, A., Li, Y., Wang, Y., Lowe, M.J., Dzemidzic, M., 2009. Resting state corticolimbic connectivity abnormalities in unmedicated bipolar disorder and unipolar depression. Psychiatry Res. 171, 189–198.

Barkhof, F., Haller, S., Rombouts, S.A.R.B., 2014. Resting-state functional MR imaging: a new window to the brain. Radiology 272, 29–49.

Coplan, J.D., Gopinath, S., Abdallah, C.G., Berry, B.R., 2014. A neurobiological hypothesis of treatment-resistant depression – mechanisms for selective serotonin reuptake inhibitor non-efficacy. Front. Behav. Neurosci. 8, 1–16.

Dichter, G.S., Gibbs, D., Smoski, M.J., 2015. A systematic review of relations between resting-state functional-MRI and treatment response in major depressive disorder. J. Affect. Disord. 172, 8–17.

Disner, S.G., Beevers, C.G., Haigh, E.A., Beck, A.T., 2011. Neural mechanisms of the

cognitive model of depression. Nat. Rev. Neurosci. 12, 467–477.
Dusi, N., Barlati, S., Vita, A., Brambilla, P., 2015. Brain structural effects of antidepressant treatment in major depression. Curr. Neuropharmacol. 13, 458–465.
Gong, Q., He, Y., 2015. Depression, neuroimaging and connectomics: a selective overview. Biol. Psychiatry 77, 223–235.
Graham, J., Salimi-Khorshidi, G., Hagan, C., Walsh, N., Goodyer, I., Lennox, B., et al., 2013. Meta-analytic evidence for neuroimaging models of depression: state or trait? J. Affect Disord. 151, 423–431.
Guo, H., Cheng, C., Cao, X., Xiang, J., Chen, J., Zhang, K., 2014. Resting-state functional connectivity abnormalities in first-onset unmedicated depression. Neural Regen. Res. 9, 153–163.
Guo, W., Liu, F., Xiao, C., Zhang, Z., Liu, J., Yu, M., et al., 2015. Decreased insular connectivity in drug-naive major depressive disorder at rest. J. Affect. Disord. 179, 31–37.
Guo, W.B., Liu, F., Xue, Z.M., Xu, X.J., Wu, R.R., Ma, C.Q., et al., 2012. Alterations of the amplitude of low-frequency fluctuations in treatment-resistant and treatment-response depression: a resting-state fMRI study. Prog. Neuropsychopharmacol. Biol. Psychiatry 37, 153–160.
Han, Y., Wang, J., Zhao, Z., Min, B., Lu, J., Li, K., et al., 2011. Frequency-dependent changes in the amplitude of low-frequency fluctuations in amnestic mild cognitive impairment: a resting-state fMRI study. NeuroImage 55, 287–295.
Ionescu, D.F., Rosenbaum, J.F., Alpert, J.E., 2015. Pharmacological approaches to the challenge of treatment-resistant depression. Dialogues Clin. Neurosci. 17, 111–126.
Jentsch, M.C., Van Buel, E.M., Bosker, F.J., Gladkevich, A.V., Klein, H.C., Oude Voshaar, R.C., et al., 2015. Biomarker approaches in major depressive disorder evaluated in the context of current hypotheses. Biomark. Med. 9, 277–297.
Kaiser, R.H., Andrews-Hanna, J.R., Wager, T.D., Pizzagalli, D.A., 2015. Large-scale network dysfunction in major depressive disorder: a meta-analysis of resting-state functional connectivity. JAMA Psychiatry 72, 603–611.
Kerestes, R., Davey, C.G., Stephanou, K., Whittle, S., Harrison, B.J., 2014. Functional brain imaging studies of youth depression: a systematic review. Neuroimage Clin. 4, 209–231.
Klauser, P., Fornito, A., Lorenzetti, V., Davey, C.G., Dwyer, D.B., Allen, N.B., et al., 2015. Cortico-limbic network abnormalities in individuals with current and past major depressive disorder. J. Affect. Disord. 173, 45–52.
Krusemark, E., Novak, L., Gitelman, D., Li, W., 2013. When the sense of smell meets emotion: anxiety-state-dependent olfactory processing and neural circuitry adaptation. J. Neurosci. 33, 15324–15332.
Li, B., Liu, L., Friston, K.J., Shen, H., Wang, L., Zeng, L.L., et al., 2013. A treatment-resistant default mode subnetwork in major depression. Biol. Psychiatry 74, 48–54.
Lui, S., Wu, Q., Qiu, L., Yang, X., Kuang, W., Chan, R.C., et al., 2011. Resting-state functional connectivity in treatment-resistant depression. Am. J. Psychiatry 168, 642–648.
Luo, Q., Deng, Z., Qin, J., Wei, D., Cun, L., Qiu, J., et al., 2015. Frequency dependant topological alterations of intrinsic functional connectome in major depressive disorder. Sci. Rep. 5, 9710.
Maletic, V., Raison, C., 2014. Integrated neurobiology of bipolar disorder. Front. Psychiatry 5, 1–24.
Malykhin, N.V., Coupland, N.J., 2015. Hippocampal neuroplasticity in major depressive disorder. Neuroscience 309, 200–213.
Marchetti, I., Koster, E.H., Sonuga-Barke, E.J., De Raedt, R., 2012. The default mode network and recurrent depression: a neurobiological model of cognitive risk factors. Neuropsychol. Rev. 22, 229–251.
Mingtian, Z., Shuqiao, Y., Xiongzhao, Z., Jinyao, Y., Xueling, Z., Xiang, W., et al., 2012. Elevated amygdala activity to negative faces in young adults with early onset major depressive disorder. Psychiatry Res. 201, 107–112.
Minor, K.L., Champion, J.E., Gotlib, I.H., 2005. Stability of DSM-IV criterion symptoms for major depressive disorder. J. Psychiatr. Res. 39, 415–420.
Murray, E.A., Wise, S.P., Drevets, W.C., 2011. Localization of dysfunction in major depressive disorder: prefrontal cortex and amygdala. Biol. Psychiatry 69, 43–54.
Palazidou, E., 2012. The neurobiology of depression. Br. Med. Bull. 101, 127–145.
Posner, J., Hellerstein, D.J., Gat, I., Mechling, A., Klahr, K., Wang, Z., et al., 2013. Antidepressants normalize the default mode network in patients with dysthymia. JAMA Psychiatry 70, 373–382.
Ruge, H., Wolfensteller, U., 2015. Distinct contributions of lateral orbito-frontal cortex, striatum, and fronto-parietal network regions for rule encoding and control of memory-based implementation during instructed reversal learning. NeuroImage 125, 1–12.
Saad, Gotts SJ., Murphy, K., Chen, G., Jo, H., Martin, A., et al., 2012. Trouble at rest: how correlation patterns and group differences become distorted after global signal regression. Brain Connect. 2, 25–32.
Santos, M., Carvalho, S., Lima, L., Mota-Pereira, J., Pimentel, P., Maia, D., et al., 2015. FAS -670A>G genetic polymorphism is associated with treatment resistant depression. J. Affect. Disord. 185, 164–169.
Sawaya, H., Johnson, K., Schmidt, M., Arana, A., Chahine, G., Atoui, M., et al., 2015. Resting-state functional connectivity of antero-medial prefrontal cortex subregions in major depression and relationship to emotional intelligence. Int. J. Neuropsychopharmacol. 18, 1–27.
Schablitzky, S., Pause, B., 2014. Sadness might isolate you in a non-smelling world: olfactory perception and depression. Front. Psychol. 5, 1–20.
Shad, M.U., Bidesi, A.P., Chen, L.-A., Ernst, M., Rao, U., 2011. Neurobiology of decision making in depressed adolescents: a functional magnetic resonance imaging study. J. Am. Acad. Child Adolesc. Psychiatry 50, 612–621.
Vincent, J.L., Kahn, I., Snyder, A.Z., Raichle, M.E., Buckner, R.L., 2008. Evidence for a frontoparietal control system revealed by intrinsic functional connectivity. J. Neurophysiol. 100, 3328–3342.
Wang, L., Hermens, D.F., Hickie, I.B., Lagopoulos, J., 2012. A systematic review of resting-state functional-MRI studies in major depression. J. Affect Disord. 142, 6–12.
Wang, Y.-L., Yang, S.-Z., Sun, W.-L., Shi, Y.-Z., Duan, H.-F., 2016. Altered functional interaction hub between affective network and cognitive control network in patients with major depressive disorder. Behav. Brain Res. 298, 301–309.
Whitton, A.E., Treadway, M.T., Pizzagalli, D.A., 2014. Reward processing dysfunction in major depression, bipolar disorder and schizophrenia. Curr. Opin. Psychiatry 28, 7–12.
Wu, Q.Z., Li, D.M., Kuang, W.H., Zhang, T.J., Lui, S., Huang, X.Q., et al., 2011. Abnormal regional spontaneous neural activity in treatment-refractory depression revealed by resting-state fMRI. Hum. Brain Mapp. 32, 1290–1299.
Yu, R., Chien, Y.L., Wang, H.L., Liu, C.M., Liu, C.C., Hwang, T.J., et al., 2014. Frequency-specific alternations in the amplitude of low-frequency fluctuations in schizophrenia. Hum. Brain Mapp. 35, 627–637.
Zalesky, A., Fornito, A., Bullmore, E.T., 2010. Network-based statistic: identifying differences in brain networks. Neuroimage 53, 1197–1207.
Zalesky, A., Fornito, A., Egan, G.F., Pantelis, C., Bullmore, E.T., 2012. The relationship between regional and inter-regional functional connectivity deficits in schizophrenia. Hum. Brain Mapp. 33, 2535–2549.
Zalesky, A., Fornito, A., Seal, M.L., Cocchi, L., Westin, C.F., Bullmore, E.T., et al., 2011. Disrupted axonal fiber connectivity in schizophrenia. Biol. Psychiatry 69, 80–89.
Zeng, L., Shen, H., Liu, L., Wang, L., Li, B., Fang, P., et al., 2012. Identifying major depression using whole-brain functional connectivity: a multivariate pattern analysis. Brain A J. Neurol. 135, 1498–1507.
Zuo, X.-N., Di Martino, A., Kelly, C., Shehzad, Z.E., Gee, D.G., Klein, D.F., et al., 2010. The oscillating brain: complex and reliable. NeuroImage 49, 1432–1445.